URSI GASS 2020, Rome, Italy, 29 August - 5 September 2020

Low Mutual Coupling Dual-port Dual-band MIMO Antenna Array for Mobile Terminal

Mohit Mishra*(1), Rakhesh Singh Kshetrimayum(1), and Sumantra Chaudhuri(1)
(1) Department of Electronics and Electrical Engineering, Indian Institute of Technology, Guwahati, India-781039

Abstract

A dual-port dual-band multiple-input-multiple-output (MIMO) antenna array comprises of two printed circular monopole antennas is presented. Based on simulated data, the -10 dB impedance bandwidth of the antenna is noted from 2.3 GHz to 2.8 GHz and 3.37 GHz to 3.72 GHz. The isolation between the antenna elements is enhanced by connecting antennas through a microstrip neutralisation line along with a stub in the ground plane. Mutual coupling is found to be below -15 dB with an inter-element spacing of 0.092 times the free-space wavelength at 2.3 GHz. The maximum gain of the antenna is noted to be 3.66 dBi with an envelope correlation coefficient $\leq$ 0.06211 in its entire bandwidth.

1 Introduction

Multiple-input-multiple-output (MIMO) is a modern communication system technology that can meet the requirements of high throughput and good quality communication. MIMO implementation requires multiple antennas on the transmitter and receivers front end modules. For judicious space utilization and compactness, antennas must be placed as close as possible, but it leads to increased electromagnetic interaction between antenna elements. Therefore, mutual coupling becomes a problem in compact MIMO antennas. Mutual coupling is highly undesirable [1, 2, 3, 4] because it can degrade the signal to interference ratio. It can also lead to the wrong estimation of the carrier frequency offset [5] and incorrect channel estimation [6]. With the advancement in the communication services, mobile terminal with multi-standard compatibility is the need of the hour. Therefore, to design low-mutual coupling multiple frequency band MIMO antenna array with a decreased overall footprint is a popular topic among antenna engineers.

In literature, several methods have been proposed to reduce the mutual coupling between antenna elements [7-12]. A slot in the ground plane is used as a defected ground structure in between the microstrip patches to mitigate the interaction between antennas in [7]. In [8], a tree-shaped structure in the ground plane is used to decouple two monopoles and a T-shaped grounded branch is used to suppress the coupling between the two orthogonal monopole antennas in [9]. A miniaturized two-layer electromagnetic band gap (EBG) structures are presented for reducing the electromagnetic coupling between closely spaced ultra wideband (UWB) planar monopoles in [10]. Neutralisation line (NL) for the mutual coupling mitigation is used in [11] for the very first time to decouple two PIFAs. An NL is inserted between the coupling elements to increase the port to port isolation in [12], while a combination of the grounded branch and neutralisation line (NL) techniques have been used together in [13].

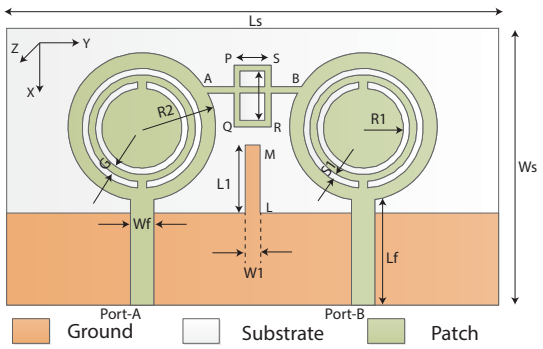

Figure 1. Antenna geometry and design specifications (mm)

In this paper, a two-port MIMO antenna comprising of two circular printed monopole antennas with dual-band characteristics is presented. The isolation between the antenna elements is enhanced by connecting the antenna elements through a simple neutralisation line AB with an additional rectangular loop in it and a stub LM in the ground plane as depicted in Fig. 1. Isolation between antenna elements is found to be more than 15 dB in the operating frequency range.

2 Antenna Geometry

A two-element microstrip antenna array comprising of two circular microstrip monopole antennas with its schematic information is shown in Fig. 1. The top layer consists of two circular patches with split ring-

shaped slots. Each antenna element is fed by a separate microstrip line attached to these patches. The antenna design uses RT-Duroid 5870 substrate with dielectric constant of 2.33 and 1.57 mm thickness. Antenna elements are connected with the neutralisation lines AB with an additional rectangular loop PQRS in the top layer and one stub LM which is extended in the ground plane between the radiators and is referred to as the grounded stub (GS). Various design parameter are as follows: Ls = 80 mm, Ws = 45 mm, Lf = 17 mm, Wf = 3.8 mm, L1 = 11 mm, W1 = 2.5 mm, R1 = 6.5 mm, R2 = 12 mm, G = 1.2 mm, S1 = 1 mm, PS = QR = 6 mm, PQ = SR = 10 mm.

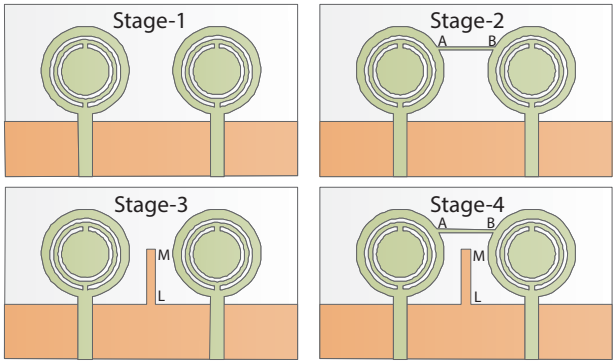

Figure 2. Intermediate design stages before the final design

3 Working Mechanism

In this antenna array, circular patches loaded with split-ring shaped slots are used as radiating elements. This antenna design is evolved through various design stages, as shown in Fig. 2. When the array is simulated without any decoupling units i.e. stage-1, the S-parameters are shown in Fig. 3a. $|S_{11}|$ are found to be good but the isolation between antenna elements is observed to be $\leq$ 10 dB in the lower band and $\leq$ 15 dB in the upper band, which is quite low. To reduce the electromagnetic interaction between antennas, antennas are connected with a neutralisation line (AB) as shown in stage-2 which is capable of enhancing the isolation in 2.5 GHz band but unable to reduce the mutual coupling in the 3.5 GHz band. Stage-3 examines the capability of the grounded stub LM which is $\lambda_g/4$ in length at 3.5 GHz. It is observed from the S-parameters of stage-3 that the mutual coupling in 3.5 GHz band can be reduced by extending a $\lambda_g/4$ long stub in the ground plane referred to as grounded stub. This grounded stub is capable of reducing the mutual coupling below -15 dB only in 3.5 GHz band and not in 2.5 GHz band. This is quite visible in the S-parameters corresponding to the stage-3 design. Observing the role of the neutralisation line AB and grounded branch LM for the mutual coupling reduction at 2.5 GHz and 3.5

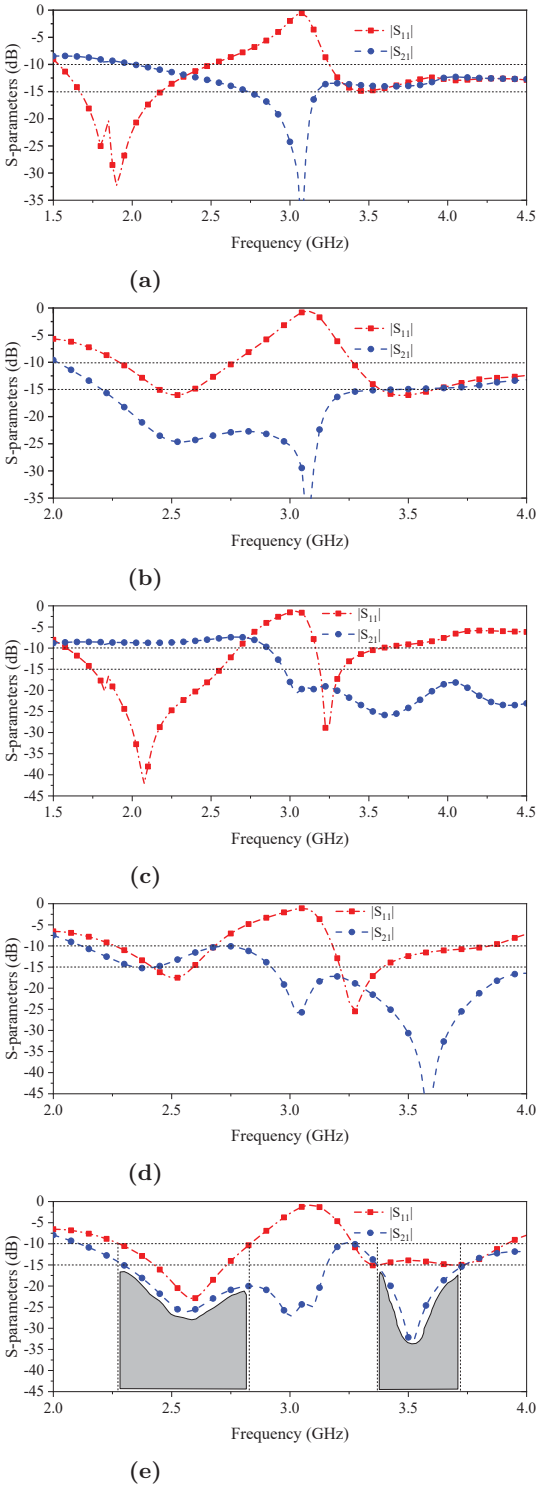

Figure 3. S-parameters (a) Stage-1 (b) Stage-2 (c) Stage-3 (d) Stage-4 (e) Final stage

GHz band respectively, an attempt to reduce the mutual coupling in both the bands is done by combining the previous stages and stage-4 is evolved out of it. It can be seen in the figure 3d that NL and GS together

is not capable of reducing the mutual coupling below 15 dB in both the bands. With both NL and GS, the isolation characteristics is good only in the 3.5 GHz band while both $|S_{11}|$ and $|S_{21}|$ becomes poorer in the 2.5 GHz band as compared to second stage. In order to achieve good characteristics in both bands, i.e. the final design, the stage-4 design is modified by connecting the additional rectangular loop PQRS to NL, which provides two more paths (A-P-S-B, A-Q-R-B) in addition to AB. It is observed that with a slight reduction in the length of the grounded stub LM and placement of the rectangular loop with the neutralisation line, mutual coupling in both the bands falls below -15 dB with a minimum mutual coupling of -25 dB in 2.5 GHz band and -32 dB in the 3.5 GHz band. The frequency range where $|S_{11}|$ is $\leq$ -10 dB and $|S_{21}| \leq$ -15 dB, is shaded with the gray colour in Fig. 3e.

4 Results

The measured $|S_{11}|$, $|S_{21}|$ along-with their simulated values are plotted as functions of frequency in Fig. 5. The -10 dB simulated impedance bandwidth of the antenna lies between 2.3 GHz GHz to 2.825 GHz and 3.375 GHz to 3.725 GHz, and isolation between antenna elements is found to be more than 15 dB. However, the -10 dB measured impedance bandwidth of the fabricated prototype is noted from 2.4 GHz to 2.84 GHz and 3.5 GHz to 3.95 GHz. The measured isolation is greater than 10 dB from 2.55-2.84 GHz and 3.5-3.95 GHz, and for the frequency range from 2.55 -2.84 GHz and 3.5-3.65 GHz, isolation is noted to be higher than 15 dB with maximum isolation of 23.98 dB in 2.6 GHz band and 20 dB in 3.5 GHz band. The mismatch in the simulated and measured S-parameters is generally because of the tolerances in the fabrication and measurement process.

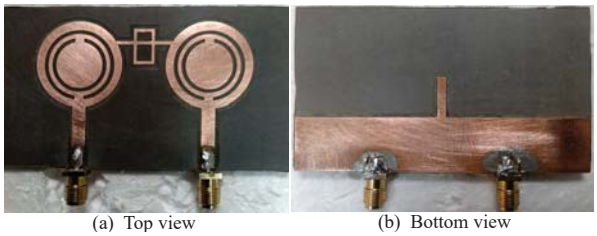

(a) Top view (b) Bottom view

Figure 4. Fabricated prototype

The simulated and measured radiation pattern of the proposed antenna for $\phi = 0^0$ and $\phi = 90^0$ planes at 2.6 GHz and 3.5 GHz are plotted in Fig. 6. During pattern measurement, only port-B is excited while port-A is terminated with the 50 Ω matched load. The radiation pattern corresponding to port-A is the mirror image of the radiation pattern corresponding to port-B, thus exhibiting pattern diversity. Therefore, the radiation pattern corresponding to only port-B is plotted. The

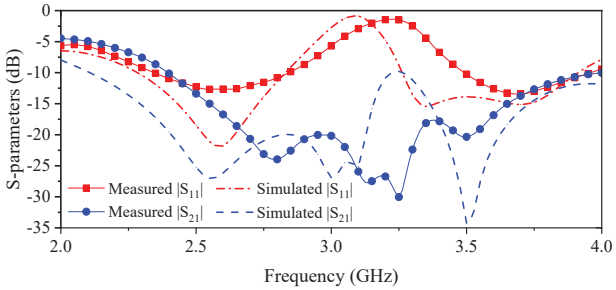

Figure 5. Simulated and measured S-parameters

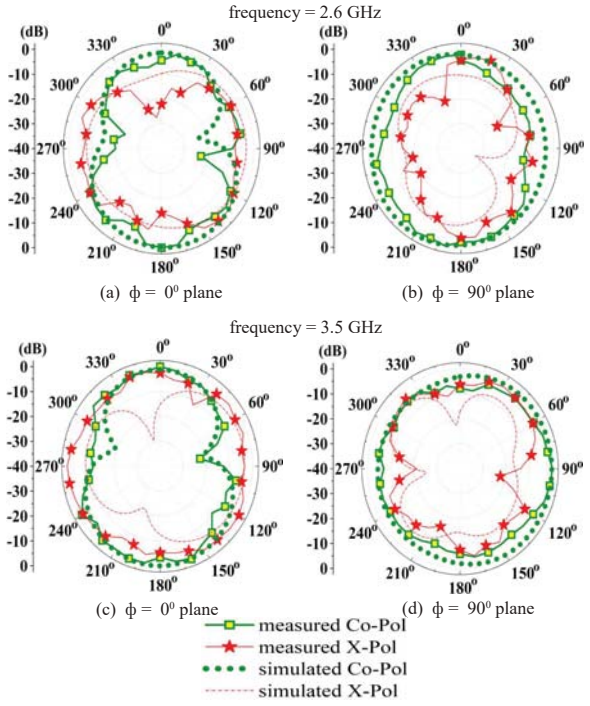

Figure 6. Radiation pattern

measured gain versus frequency plot is shown in Fig. 7 and maximum gain of the antenna is noted to be 3.66 dBi.

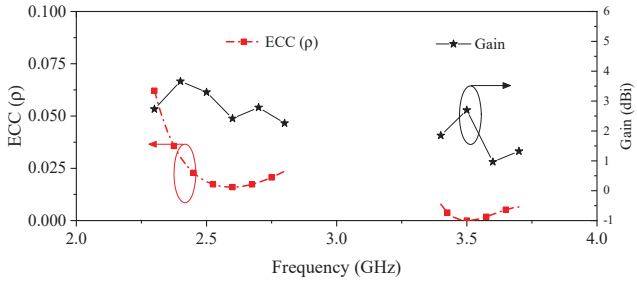

Figure 7. ECC and measured gain

The envelope correlation coefficient (ECC) and diversity gain (DG) are important parameters to be con-

sidered in the MIMO communication systems. ECC is calculated using (1) in [14].

$$\rho_{ij} = \frac{\left| \iint_{4\pi} \left[\vec{F}_i(\theta,\phi) * \vec{F}_j(\theta,\phi) \right] d\Omega \right|^2}{\left(\iint_{4\pi} \left| \vec{F}_i(\theta,\phi) \right|^2 d\Omega \right) \left(\iint_{4\pi} \left| \vec{F}_j(\theta,\phi) \right|^2 d\Omega \right)} \tag{1}$$

$$\mathrm{DG} = 10\sqrt{1 - |0.99\rho|^2} \tag{2}$$

Here, $\vec{F}_i(\theta,\phi)$ is the 3-D radiation field of the antenna when the i^{th} port is excited and Ω is the solid angle. ECC curve against frequency for both the frequency bands is plotted in Fig. 7 and noted to be ≤ 0.06211. The diversity gain (DG) is evaluated using (2) in [14]. The calculated DG for the highest ECC across bandwidth is greater than 9.98 dB.

5 Conclusion

A low mutual coupling dual-port, dual-band MIMO antenna is designed, fabricated and tested. Mutual coupling in both the frequency bands (2.3-2.8 GHz and 3.3-3.7 GHz) is reduced with a modified neutralisation line and a grounded stub together. This antenna has a bandwidth from 2.3 GHz GHz to 2.8 GHz and 3.37 GHz to 3.72 GHz and covers 2.4 GHz-WLAN, LTE 38, LTE 40, LTE 41, 3.5 GHz-WiMAX and 3.3 GHz to 3.7 GHz for 5G applications. The radiation patterns are plotted, and a maximum gain of 3.66 dBi is noted in the operating frequency range of the antenna. Isolation is found to be greater than 15 dB, and the envelope correlation coefficient is noted to be less than 0.06211. Therefore, this antenna confirms its suitability for multiple band MIMO applications.

References

[1] X. Chen, S. Zhang, and Q. Li, "A review of mutual coupling in mimo systems," *IEEE Access*, vol. 6, pp. 24 706–24 719, May 2018.

[2] M. A. Jensen and J. W. Wallace, "A review of antennas and propagation for MIMO wireless communications," *IEEE Transactions on Antennas and Propagation*, vol. 52, no. 11, pp. 2810–2824, Nov 2004.

[3] G. Bauch and A. Alexiou, "MIMO technologies for the wireless future," in *2008 IEEE 19th International Symposium on Personal, Indoor and Mobile Radio Communications*. IEEE, pp. 1–6, 2008.

[4] M. S. Sharawi, "Printed multi-band MIMO antenna systems and their performance metrics [wireless corner]," *IEEE Antennas and Propagation Magazine*, vol. 55, no. 5, pp. 218–232, Oct 2013.

[5] Y. Wu, J. Bergmans, and S. Attallah, "Effects of antenna correlation and mutual coupling on the carrier frequency offset estimation in MIMO systems," in *2010 6th International Conference on Wireless Communications Networking and Mobile Computing (WiCOM)*. IEEE, pp. 1–4, 2010.

[6] S. Lu, H. T. Hui, M. E. Bialkowski, X. Liu, H. Lui, and N. Shuley, "The effect of antenna mutual coupling on channel estimation of MIMO-OFDM systems," in *2007 IEEE Antennas and Propagation Society International Symposium*. IEEE, pp. 2945–2948, 2007.

[7] J. OuYang, F. Yang, and Z. Wang, "Reducing mutual coupling of closely spaced microstrip MIMO antennas for WLAN application," *IEEE Antennas and Wireless Propagation Letters*, vol. 10, pp. 310–313, 2011.

[8] S. Zhang, Z. Ying, J. Xiong, and S. He, "Ultrawideband MIMO/diversity antennas with a tree-like structure to enhance wideband isolation," *IEEE Antennas and Wireless Propagation Letters*, vol. 8, pp. 1279–1282, 2009.

[9] C. Yang, Y. Yao, J. Yu, and X. Chen, "Novel compact multiband MIMO antenna for mobile terminal," *International Journal of Antennas and Propagation*, vol. 2012, 2012.

[10] Q. Li, A. P. Feresidis, M. Mavridou, and P. S. Hall, "Miniaturized double-layer EBG structures for broadband mutual coupling reduction between UWB monopoles," *IEEE Transactions on Antennas and Propagation*, vol. 63, no. 3, pp. 1168–1171, 2015.

[11] A. Diallo, C. Luxey, P. Le Thuc, R. Staraj, and G. Kossiavas, "Study and reduction of the mutual coupling between two mobile phone PIFAs operating in the DCS1800 and UMTS bands," *IEEE Transactions on Antennas and Propagation*, vol. 54, no. 11, pp. 3063–3074, 2006.

[12] A. Cihangir, F. Ferrero, G. Jacquemod, P. Brachat, and C. Luxey, "Neutralized coupling elements for MIMO operation in 4G mobile terminals," *IEEE Antennas and Wireless Propagation Letters*, vol. 13, pp. 141–144, 2014.

[13] Y. Wang and Z. Du, "A wideband printed dual-antenna system with a novel neutralization line for mobile terminals," *IEEE Antennas and Wireless Propagation Letters*, vol. 12, pp. 1428–1431, 2013.

[14] A. Boukarkar, X. Q. Lin, Y. Jiang, L. Y. Nie, P. Mei, and Y. Q. Yu, "A miniaturized extremely close-spaced four-element dual-band MIMO antenna system with polarization and pattern diversity," *IEEE Antennas and Wireless Propagation Letters*, vol. 17, no. 1, pp. 134–137, Jan 2018.